Journal of Information Systems Engineering and Management
2025, 10(21s)
e-ISSN: 2468-4376
https://www.jisem-journal.com/

Research Article

Enhanced Convolutional Neural Network Framework for Region of Interest-Based Efficient Bone Cancer Detection in Medical Imaging

[1]Sagarika Saka, [2.] Dr. Santhosh Boddupalli

[1] *Research Scholar, Department of Computer Science and Engineering, Koneru Lakshmaiah Education Foundation, Hyderabad-500075, Telangana, India. Email:sagarika.547@gmail.com*

[2.] *Assistant Professor, Department of Computer Science and Engineering Koneru Lakshmaiah Education Foundation, Hyderabad-500075, Telangana, India. Email:santhosh.boddupalli@klh.edu.in*

ARTICLE INFO

Received: 25 Dec 2024

Revised: 30 Jan 2025

Accepted: 20 Feb 2025

ABSTRACT

Bone cancer is a significant health issue that leads to severe complications and deaths worldwide. Early detection can significantly improve patient outcomes, often resulting in a complete cure. Traditional approaches to managing bone cancer can be augmented with technology-driven methods, particularly those enabled by artificial intelligence. Convolutional Neural Networks (CNNs) and their variants have proven effective in medical data analysis. However, deep learning techniques require enhancements to improve performance in cancer detection across various medical imaging modalities. In this paper, we propose a deep-learning framework that utilizes advanced CNN models for the automatic screening of bone cancer. We have enhanced both the CNN model and the ResNet-50 model, which are integral components of the proposed framework. Additionally, we introduced an algorithm called Learning-based Bone Cancer Detection (LbBCD), designed to optimize the utilization of these enhanced deep learning models to improve bone cancer detection efficiency. Our research emphasizes a Region of Interest (ROI) based approach to enhance the screening process for bone cancer. Using a benchmark dataset known as the Bone CT Scan dataset, our empirical study demonstrated that the proposed deep learning framework, integrated with enhanced CNN and ResNet-50 models, achieved remarkable performance. Specifically, the enhanced CNN model reached an accuracy of 90.90%, while the enhanced ResNet-50 model achieved an accuracy of 92.20%, outperforming state-of-the-art deep learning models. Therefore, this proposed system can be integrated into healthcare applications for automatically screening bone cancer, contributing to a clinical decision support system for healthcare professionals.

Keywords: Bone Cancer Detection, Deep Learning, Artificial Intelligence, Cancer Screening.

INTRODUCTION

An uncommon and deadly kind of cancer that starts in the bone tissue is called bone cancer. Metastatic bone cancer is the term used to describe cancer that has moved from other regions of the body to the actual bone. Osteosarcoma, which frequently affects the long bones, and Ewing sarcoma, which usually affects the pelvis or the long bones, are two of the various kinds of bone cancer. Around the world, there have been several documented incidences of tumors or bone cancer, and in certain cases, the illness has even resulted in fatalities. Therefore, it becomes essential to find them early on, as doing so can save countless lives. Nowadays, CT and MRI scans are used to diagnose tumors, and the procedure is time-consuming and expensive. Even in the age of artificial intelligence and machine learning, identifying tumors is still a laborious procedure that requires significant upfront costs for network training. Convolutional neural networks may be employed with X-ray pictures to identify malignancies in their early stages, and a variety of segmentation approaches are available. With the right treatments administered at the appropriate time, more complications can be avoided without hesitation if the tumor is identified and categorized at the appropriate time. We introduced a modified architecture to categorize the stages of bone tumors using inception modules and convolutional neural networks. To precisely identify the kind and stage of the cancer, diagnostic procedures often include imaging examinations, biopsies, and occasionally genetic testing. Depending on the exact kind and location of the tumor, treatment usually consists of radiation therapy, chemotherapy, and surgery. Improving results and properly managing the illness depend on early identification and treatment. Bone cancer is a dangerous and sometimes fatal disease for which good diagnosis and early detection are crucial to effective therapy. Bone cancer diagnosis

is a time-consuming and error-prone procedure that requires manual interpretation of medical imaging. However, it has been demonstrated that deep learning techniques are useful tools for automating the diagnosis of bone cancer.

The detection of bone metastases was enhanced by combining multimodal data [1]. It has been noted that identifying bone metastases in advanced prostate cancer at an early stage is both challenging and essential. Advancements in pathology have been demonstrated through the use of AI approaches, such as Computer-Aided Diagnosis (CADx) and CapsNet for feature extraction, particularly in the detection and classification of osteosarcoma [2]. The development of Efficient-BtrfyNet was achieved using butterfly-type networks and EfficientNet, which resulted in higher detection rates for cancer metastatic locations in whole-body bone scan image segmentation [3]. It has been observed that cancer-related bone metastases can lead to significant morbidity and mortality [4]. However, challenges still persist regarding automated lesion segmentation for accurate mechanical representation and fracture risk assessment. The link between aberrant bone development and DNA mutations has also been highlighted [5]. A biopsy is required, followed by an early diagnosis using imaging techniques and X-rays. The accuracy of cancer diagnoses can reach as high as 90.36% when automated deep learning models, such as ResNet101, are employed. The literature observed that CNN models are efficient in medical image processing, but they need further enhancements to leverage performance.

Our contributions in this paper are as follows: we propose a deep learning framework that employs advanced convolutional neural network (CNN) models for the automatic screening of bone cancer. We have enhanced both the CNN model and the ResNet-50 model, which are key components of the proposed framework. Additionally, we introduced an algorithm called Learning-based Bone Cancer Detection (LbBCD), designed to optimize the use of these enhanced deep learning models and improve the efficiency of bone cancer detection. Our research utilizes a Region of Interest (ROI) approach to enhance the screening process for bone cancer. Using a benchmark dataset known as the Bone CT Scan dataset, our empirical study demonstrated that the proposed deep learning framework, integrated with the enhanced CNN and ResNet-50 models, achieved remarkable performance. Specifically, the enhanced CNN model reached an accuracy of 90.90%, while the enhanced ResNet-50 model attained an accuracy of 92.20%, outperforming current state-of-the-art deep learning models.

The remainder of the paper is structured as follows: Section two reviews the literature on various existing methods for bone cancer detection. Section three presents the proposed methodology, detailing the underlying algorithm and enhanced deep learning models aimed at improving the bone cancer detection process. Section four provides empirical results using the benchmark dataset and compares the performance of the proposed models with state-of-the-art methods. Section five discusses the research presented in this paper and outlines the limitations of the study. Finally, section six concludes our research and offers directions for possible future work in this area.

2. RELATED WORK

There are many research contributions to the detection of different kinds of cancers using artificial intelligence-based approaches. Zhang et al. [1] enhanced by combining multimodal data. It is challenging but essential to identify bone metastases in advanced prostate cancer at an early stage. Alsubai et al. [2] advanced in pathology may be shown in the detection and classification of osteosarcoma with the use of AI approaches such as CADx and CapsNet feature extraction. Rachmati et al. [3] with the use of butterfly-type networks and EfficientNet, Efficient-BtrfyNet achieves higher detection rates for cancer metastatic locations in whole-body bone scan image segmentation. Ataei et al. [4] occurred in cancer, bone metastases result in considerable morbidity and death. Even yet, there are still issues with automated lesion segmentation for precise mechanical representation and fracture risk evaluation. Gawade et al. [5] based in DNA mutations, aberrant bone development results. A biopsy must come first, followed by an early diagnosis of the illness utilizing imaging and X-rays. Cancer diagnosis accuracy is quite high (90.36%) using automated deep-learning models such as ResNet101.

Xiong et al. [6] with excellent accuracy and generalizability across several hospital datasets, a 2.5D deep learning model trained on CT images can differentiate between osteoblastic bone metastases and bone islands. Ramasamy et al. [7] created blood, such as AML and MM types, are the source of bone marrow malignancy. Improving manual procedures is necessary, therefore a hybrid approach that incorporates deep learning produces better classification and segmentation accuracy for cancer cells. Mohseninia et al. [8] prostated cancer bone metastases are frequent and impact patient outcomes. With some tracers, imaging techniques like PET/CT and PET/MRI offer improved detection capabilities. AI and radiomics enhance accuracy, which might result in better customized medicine. Afnouch et al. [9] limited datasets present obstacles for machine learning in medical image analysis, especially for Bone Metastases (BM). Hybrid-AttUnet++ models improve segmentation accuracy using BM-Seg dataset, annotated for CT images, surpassing existing techniques. Wang et al. [10] with 96.54% accuracy, the deep learning model on MRI images is used in this work to diagnose spine metastases. This diagnosis is important for prompt patient care and therapy evaluation.

Gawade et al. [11] osteosarcoma is a bone tumor mostly affecting the long bones that is brought on by mutations in DNA. It's critical to do early imaging and X-ray detection. Deep learning models such as ResNet101, which achieve 90.36% diagnostic accuracy, enhance cancer detection capabilities. Kreem et al. [12] used Inception v3 and LSTM, a novel OSADL-BCDC approach achieves 95% accuracy in automated bone cancer identification from X-ray images, enhancing diagnostic speed and convergence. Subsequent investigations seek to improve the performance of classifiers and incorporate several imaging modalities. Goller et al. [13] differentiated between benign and malignant vertebral fractures, three-dimensional CT-based texture characteristics were retrieved using a CNN architecture. Significant differences in skewness worldwide were observed, indicating that DL-based TF extraction may be able to improve diagnostic precision in the categorization of vertebral fractures. Ibrahim et al. [14] with a focus on high specificity and sensitivity, the project intends to create a DL algorithm for metastatic bone disease classification from bone scintigraphy images. After validation, this algorithm may help radiologists during their training and in their clinical practice. Halme et al. [15] used bone scintigraphy and CNNs, transthyretin amyloidosis was accurately detected and its cardiac uptake grades were graded in this work. Automated clinical screening might benefit from the use of this method, which performed better than earlier models.

Bansal et al. [16] automated detection approach termed IF-FSM-C uses a combination of customized criteria and deep learning to identify osteosarcoma from white matter injuries (WSIs). By selecting features using BAOA-S and achieving 99.54% accuracy, it performs better than earlier methods for osteosarcoma detection. Hinzpeter et al. [17] used 68 Ga-PSMA PET as a reference, radiomics on CT images successfully distinguished between invisible bone metastases in prostate cancer patients, demonstrating the possibility of automated bone segmentation and screening for early metastasis identification. Kumar et al. [18] used SN-AM dataset and deep learning—more specifically, a Dense Convolutional Neural Network—the study's primary goal is to identify acute lymphoblastic leukemia (ALL) and multiple myeloma (MM) (DCNN). The DCNN achieved an accuracy of 97.2%, surpassing more traditional machine learning methods such as SVMs and Decision Trees. Belal et al. [19] created a CNN-based technique for bone segmentation in CT images that would achieve manual delineation-level precision. This technique is essential for automated PET/CT-based tumor burden estimation in prostate cancer. Papandrianos et al. [20] with respect to known CNN architectures in medical image analysis, this study's CNN algorithm performs better when it comes to classifying bone scintigraphy pictures for prostate cancer metastatic identification.

Shao et al. [21] used a CNN based on LeNet-5, surface-enhanced Raman spectroscopy (SERS) examined 1281 serum spectra from prostate cancer patients to identify bone metastases, demonstrating the possibility of better screening with bigger datasets. Jabber et al. [22] with 92% accuracy, an automated method for detecting bone cancer employing SVM-based M3 filtering and Fuzzy C-Means segmentation can help with early diagnosis and prompt treatment, both of which are critical for lowering mortality. Noguchi et al. [23] developed through trials on several datasets, and it demonstrated excellent accuracy for whole-body CT bone segmentation. RICAP augmentation improved the segmentation robustness by effectively preventing overfitting. Anisuzzaman et al. [24] through the use of CNN-based CADx tools, notably VGG19 and Inception V3 models trained on histological images, this work seeks to improve osteosarcoma identification. According to the results, VGG19 reached 96% accuracy, which represents a major breakthrough in automatically diagnosing cancer. Fang et al. [25] used deep convolutional neural networks (DCNNs), namely U-Net for segmentation and DenseNet-121 for BMD, the study attempted to automate the processes of segmenting the vertebral body and calculating bone mineral density (BMD) in CT scans of 1449 individuals.

Table 1: Summary of literature findings on bone cancer diagnosis

Ref	Approach	Technique	Algorithm	Dataset	Limitation
[1]	DL and AI	KNN	LASSO algorithm	Custom dataset	Improvement for more accurate guidance to doctors is still desired.
[3]	DL	Butterfly-type network	DL algorithm	Custom dataset	Post-processing is yet to be carried out.
[9]	DL	CNN	ML and DL algorithms	BM- Seg dataset	Dataset diversity to be improved for better performance in the future.
[11]	DL	RF and SVM	ResNet101 algorithm	ImageNet dataset	Exploring other DL models is yet desired.
[12]	DL and AI	OSADL-BCDC) method	Owl search algorithm	MURA dataset	Explainable AI is to be used in future.

[16]	DL	Segmentation methods	Metaheuristic algorithms	Osteosarcoma dataset	Other DL models are to be explored.
[17]	ML	Gradient boosting	ML algorithm	Custom dataset	Needs improvement of dataset to increase diversity.
[18]	DL	CNNs	Ensemble approach	SN-AM dataset	Improvement is required with diversified data and other DL models.
[24]	DL	Transfer learning techniques, pre-trained CNNs	DL algorithm	Osteosarcoma dataset	Model performance need to be evaluated with pathologists.
[29]	DL	Grad-CAM technique	DenseNet algorithm	Custom dataset	Dataset expansion and hybrid deep learning are yet to be explored.

Table 2: Datasets used in the prior works

Dataset	**Reference**
ImageNet dataset	[5], [11], [24]
gzch dataset kaggle	[6]
SN- AM dataset	[7], [18]
BM- Seg dataset	[9]
MURA dataset	[12]
CT data set	[13]
Osteosarcoma dataset	[16]
DICOM dataset	[30]
Custom dataset	[1], [3], [14], [20], [21], [22], [23], [27], [29]

Aoki et al. [26] investigated the use of a deep learning-based algorithm to identify bone metastases in patients with prostate cancer using bone scintigraphy. It compares the algorithm's effectiveness with that of nuclear medicine professionals and highlights certain drawbacks as well as the requirement for bigger, multicenter studies for validation. Vandana and Sathyavathi [27] limited scope and laborious manual techniques of classical histopathology make it difficult to diagnose diseases like bone cancer in a timely manner. Automated techniques with 92% accuracy in identifying various types of bone cancer are made possible by deep learning and digital hepatology. Masoudi et al. [28] developed a deep learning model to classify prostate cancer bone lesions as benign or malignant using CT scans from 114 individuals. It achieved 92.2% accuracy by integrating 2D ResNet-50 and 3D ResNet-18, demonstrating the importance of morphology, texture, and volumetric data in classification. He and Bi [29] enhanced the DenseNet model with Grad-CAM for the categorization of giant cell tumors and spinal osteosarcoma, obtaining 85.61% accuracy, with the goal of improving diagnostic precision and clinical decision-making in medical imaging. Park and Bom [30] with the development of AI, bone scintigraphy—which is essential to nuclear medicine—continues to change. Similar to CNNs and STEGO, deep learning holds promise for improving the accuracy and productivity of picture analysis. Table 1 shows a summary of literature findings on bone cancer detection methods while Table 2 shows datasets used in prior works. From the literature review, it was observed that CNN models are efficient, but they need further enhancement to serve different imaging modalities.

3. MATERIALS AND METHODS

This section outlines the proposed methodology and materials, including the deep learning framework, the enhanced CNN model, the enhanced ResNet-50 model, algorithm details, dataset information, and performance evaluation methodology.

3.1 Methods

Over methodology focuses on enhancing deep learning models to improve efficiency in medical image analysis. In an empirical study, bone CT scan images were utilized, and enhanced convolutional neural network (CNN) models were developed to process these images effectively for the detection of bone cancer. The proposed deep

learning framework, illustrated in Figure 1, includes mechanisms for bone cancer screening through a supervised learning approach. This framework is equipped with advanced deep-learning models aimed at enhancing its capabilities. The framework illustrates a proposed system for bone cancer detection using medical imaging, specifically bone CT scan images. The process begins with the collection of a bone CT scan dataset, which serves as the primary input for the system. These images likely contain various bone structures, with some exhibiting potential signs of bone cancer. The dataset is then subjected to a pre-processing stage, where the images are prepared for further analysis. This stage may involve operations such as resizing, normalization, noise reduction, and augmentation, ensuring that the images are in an optimal format for training the deep learning model. Proper pre-processing helps improve the model's accuracy and efficiency.

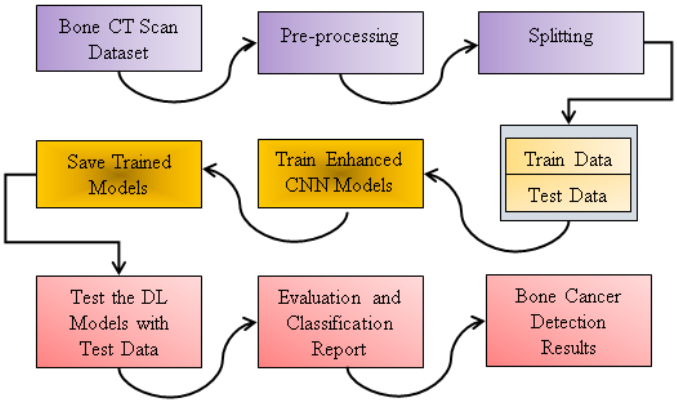

Figure 1: Proposed framework for bone cancer detection in medical imaging (bone CT scan images)

After pre-processing, the dataset is split into two parts: training data and test data. The training data is used to teach the model to recognize patterns that may indicate the presence of bone cancer, while the test data is held out for later evaluation. This division of data helps to assess how well the model generalizes to new, unseen data and prevents overfitting, where the model performs well on training data but poorly on new inputs. Once the dataset is split, the next stage involves training enhanced convolutional neural network (CNN) models. These models are specially designed to detect cancerous features in medical images by leveraging deep learning techniques. The training process involves adjusting the weights and biases of the CNN layers to minimize the error between the predicted outcomes and the actual labels (cancerous or non-cancerous). Over time, the enhanced CNN models become more capable of identifying subtle patterns in the bone CT scans that are indicative of cancer.

Once the model is trained, it is saved for future use. This allows the system to quickly load the trained models without requiring retraining, making the system more efficient in practical applications. The saved models are then tested using the test data, which has not been exposed to the model during training. This testing phase is crucial for determining the real-world performance of the model. The test results provide insight into how accurately the model can classify new images as either cancerous or non-cancerous. Following the testing phase, the system generates an evaluation and classification report. This report likely includes performance metrics such as accuracy, precision, recall, and the F1-score. These metrics help evaluate the model's ability to correctly identify cancer cases while minimizing false positives and false negatives. The classification report also provides a detailed breakdown of the model's performance, which is valuable for understanding how the model behaves in different scenarios. Finally, the evaluation results are used to produce bone cancer detection results. These results can guide medical professionals in making informed decisions regarding diagnosis and treatment. The overall system, from dataset preparation to cancer detection, is designed to automate and enhance the diagnostic process, potentially improving the accuracy and speed of bone cancer detection in medical settings.

3.2 Enhanced CNN Model

We enhanced the CNN model, shown in Figure 2, to improve its capabilities in processing bone CT scan images toward bone cancer detection. The model begins by applying two consecutive convolutional layers, each with 32 filters and a kernel size of 5x5. These layers use the 'Same' padding method to preserve the spatial dimensions of the input and employ the ReLU activation function to introduce non-linearity into the model. The first convolutional layer specifies the shape of the input images to the model, and the ReLU activation function is applied to ensure that only the positive values of the convolved results are carried forward. The two consecutive convolutional layers help the model detect basic features such as edges or textures in the CT scan images.

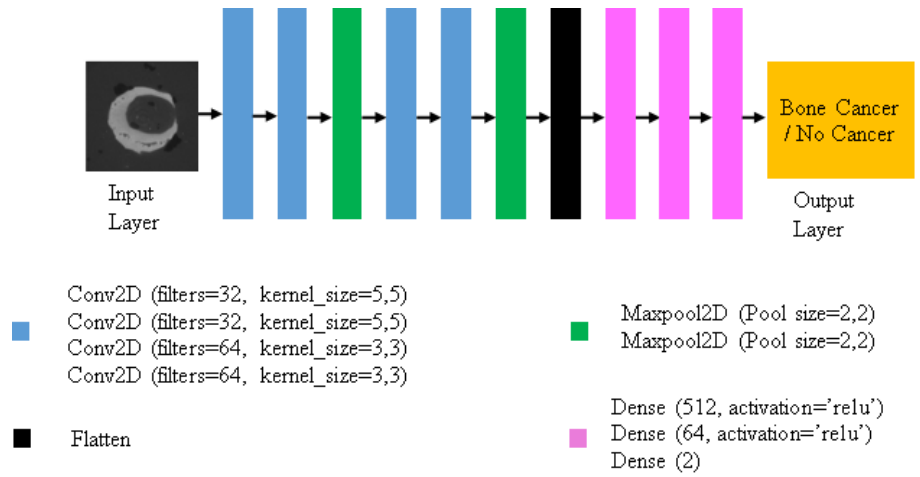

Figure 2: Enhanced CNN model for bone cancer detection in medical imaging

Following the first two convolutional layers, a MaxPooling layer is applied with a pool size of 2x2. This down-samples the image by taking the maximum value from each 2x2 window, reducing the spatial dimensions of the feature maps while retaining the most significant features. This pooling layer helps the model become more computationally efficient and prevents overfitting by reducing the size of the feature maps. Although dropout layers (commented out in the code) are not currently used, they could be added to further help with overfitting by randomly turning off a percentage of neurons during training.

The next two convolutional layers, both with 64 filters and kernel sizes of 3x3, are applied to extract more complex and detailed features. With more filters, the model is now learning more nuanced patterns, which can help identify intricate details of bone structures or possible signs of bone cancer. Again, the 'Same' padding ensures the output size remains the same, while ReLU activation continues to bring non-linearity into the network. After the second set of convolutional layers, another MaxPooling layer is added, this time with strides of 2x2, which further reduces the dimensionality of the feature maps. This pooling is essential for focusing the network on the most relevant parts of the image while discarding less important information.

Once the convolutional and pooling layers have been applied, the feature maps are flattened into a one-dimensional vector, which is then passed through two fully connected (dense) layers. The first dense layer contains 512 neurons and uses the ReLU activation function. This layer acts as a high-level reasoning layer, combining the features learned by the previous convolutional layers into a more abstract representation. The next dense layer has 64 neurons and also uses ReLU activation to continue refining the representation of the input image. Finally, the output layer contains two neurons, which likely correspond to the two possible classes: cancerous and non-cancerous. This layer is responsible for providing the final classification output of the model. The absence of an activation function in this layer suggests that a softmax or sigmoid function might be applied during the training process to interpret the two outputs as probabilities for the two classes. The enhanced CNN model is designed to extract both low-level and high-level features from bone CT scan images, combining them to detect whether bone cancer is present. By leveraging multiple convolutional layers with increasing filter sizes, pooling, and dense layers, the model is structured to handle the complexity of medical images and provide accurate classification results.

In the enhanced CNN model, the convolution operation is expressed in Eq. 1, where k is the kernel size, m, and n are the indices within the kernel, and i and j are the spatial coordinates in the input.

$$Output(i,j) = \sum_{m=o}^{k-1} \sum_{n=o}^{k-1} Input(i+m, j+n) \cdot Kernel(m,n) \quad (1)$$

The ReLU activation function, expressed in Eq. 2, treats negative values as zeros towards bringing about non-linearity in the model.

$$ReLU(x) = max(O, x) \quad (2)$$

The max pooling layer involves an operation expressed as in Eq. 3 where pool_size defines the size of the pooling window, typically 2×2.

$$Output(i,j) = Input(i+m, j+n) \quad (3)$$

The flatten layer involves in flatten operation, expressed in Eq. 4, that converts a 2D matrix into 1D vector where -1 infers the size of the second dimension automatically based on the input size.

$$Flattened\_output = reshape(Input, [batch\_size, -1]) \quad (4)$$

The fully connected layers produce output as expressed in Eq. 5 where W is the weight matrix, b is the bias vector and $ReLU$ activation function is applied to introduce non-linearity. The customized loss function used in the model is expressed as in Eq. 6 where N is the number of samples, x_i, y_i are the true coordinates and $\hat{x}_i$,$\hat{y}_i$ are the predicted coordinates. The model exploits Adam optimizer where parameter update is done as in Eq. 6 where α is the learning rate θ_t are the parameters at time step t, $\hat{m}_t$ and $\hat{v}_t$ are the bias-corrected first and second moment estimates and ϵ is a small constant to prevent division by zero.

$$\theta_{t+1} = \theta_t - \alpha \cdot \frac{\hat{m}_t}{\sqrt{\hat{v}_t + \epsilon}} \qquad (6)$$

Hyperparamter tuning is carried out for the enhanced CNN model. The tuned parameters include batch size set to 64, number of epochs set to 20 and learning rate for Adam optimizer is set to 0.001.

3.3 Enhanced ResNet50 Model

Based on the amazing modality for which research is carried out in this paper, the resonate 50 model, which is one of the pre-trained models, is enhanced with the modified architecture as presented in Figure 3.

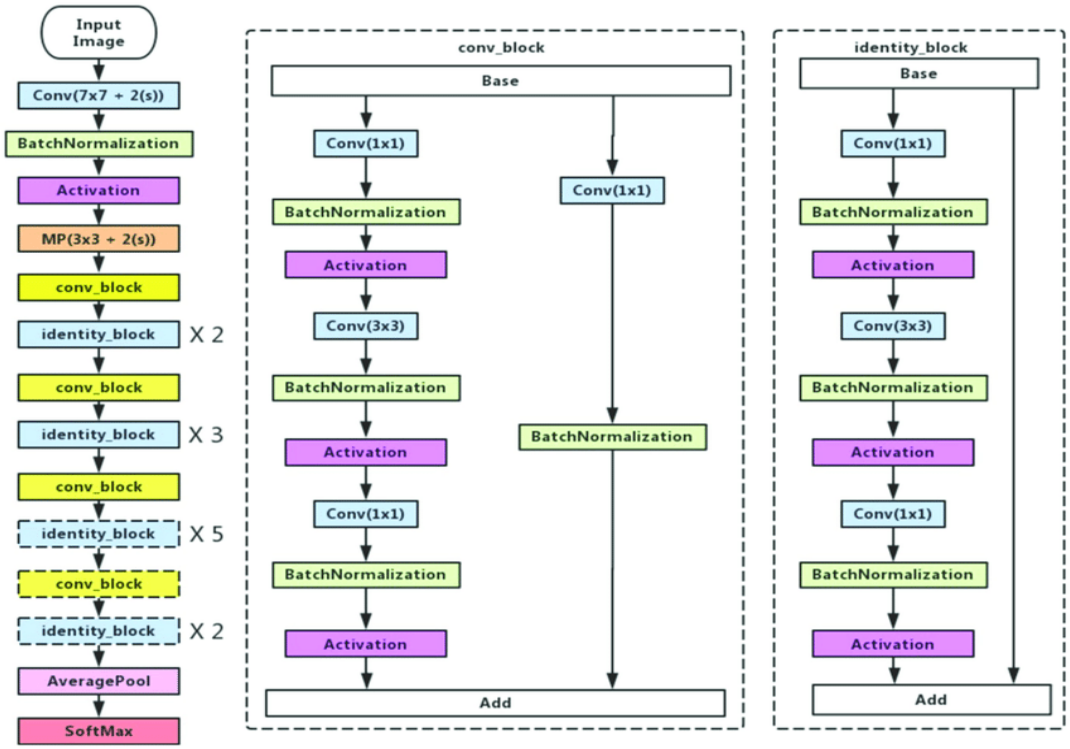

Figure 3: Enhanced architecture of ResNet50

The architecture represents an enhanced version of the ResNet50 model specifically optimized for efficient bone cancer detection. ResNet50 is a widely used deep convolutional neural network (CNN) model, well-known for its residual learning framework that allows for deeper networks without suffering from vanishing gradients. However, for a specialized task like bone cancer detection, certain enhancements and optimizations are essential to improve its performance, accuracy, and efficiency. The input image in the enhanced model is optimized for medical imaging modality CT scans. Preprocessing techniques such as contrast enhancement, noise reduction, or normalization are applied to improve the visibility of cancer-related anomalies. These preprocessing steps ensure that the model focuses on clinically significant features that distinguish normal bone structures from cancerous growths.

The use of a large initial convolution filter (7x7 with stride 2) allows the model to capture broad, contextual information from the image at the very first layer, important for recognizing general bone structures. It helps in making the model robust to different sizes, shapes, and orientations of tumors or lesions. The core of ResNet50 is the use of residual blocks, where the input is passed through convolutional layers and then added back to the output through skip connections. This design allows for the deeper network to preserve the gradient flow during backpropagation, which enables the model to learn complex hierarchical features effectively. In bone cancer detection, where precise feature extraction from deep layers is critical, residual learning prevents loss of important gradient information related to tumor characteristics. In the enhanced model, the Conv Block and Identity Block structure has been fine-tuned with a varying number of repetitions at different stages (2, 3, 5, and 2 repetitions of blocks). This modification increases the model's capacity to focus on different levels of detail,

capturing both the macro and micro features of bone and tumor tissues. The deeper layers are particularly sensitive to minute changes in bone structure, aiding in better cancer detection.

While the original ResNet50 architecture was designed for general image classification tasks (e.g., ImageNet), enhancements to the filter configurations and layer depths are introduced to make the network more sensitive to the kinds of patterns found in medical images. These may include high-pass filters that help detect edges or boundaries of bone tumors, and specialized kernels that enhance contrast in tumor regions. Bone cancer often manifests as subtle changes in bone density, structure, or texture, which require deeper and more specialized feature extraction layers. The added depth in this enhanced model allows for multi-scale feature extraction, enabling the network to differentiate between benign and malignant bone lesions, including early-stage cancers.

Regularization techniques such as dropout or weight decay may be applied to prevent overfitting when dealing with smaller medical datasets (common in specialized domains like bone cancer). These methods ensure the model generalizes well to new, unseen bone cancer images by preventing it from memorizing irrelevant details. The enhanced model utilizes batch normalization layers after every convolutional layer, which helps stabilize and accelerate training by normalizing the feature maps. In medical imaging tasks, where variability in image intensity or noise is common, batch normalization ensures that the model can converge more efficiently and focus on the patterns relevant to cancer diagnosis. In medical imaging, especially for bone cancer diagnosis, the dataset is often imbalanced, with many more images of healthy bone than of cancerous lesions. The model is enhanced by using customized loss functions, such as a weighted cross-entropy or focal loss, to give more importance to the minority class (cancerous samples) and reduce the bias towards healthy classes. This adjustment improves the model's ability to detect cancer even in rare cases.

To enhance the performance of the ResNet50 model for bone cancer detection, transfer learning is employed. The model is first pre-trained on a large, diverse dataset like ImageNet, which gives it a strong foundation in recognizing general patterns. Afterward, the model is fine-tuned on a much smaller, specific dataset of bone cancer images. This approach allows the model to leverage the learned general features while adapting them to the unique characteristics of bone cancer, such as bone irregularities, lesions, and tumors. The final layers of the network include a global average pooling layer followed by a softmax layer for classification. In the context of bone cancer detection, these layers produce probabilities that indicate whether a given input image contains cancerous tissue. The global average pooling helps reduce overfitting by summarizing feature maps, while the softmax function outputs probabilities across different classes (e.g., normal, benign, malignant). The enhanced ResNet50 model optimized for bone cancer detection incorporates several modifications that make it more suitable for medical imaging tasks. These include deeper convolutional layers for extracting fine details from bone structures, customized loss functions to handle imbalanced datasets, and transfer learning for efficient training. These enhancements allow the model to capture complex patterns related to bone cancer and improve diagnostic performance, making it a powerful tool for early and accurate detection of bone malignancies in clinical practice.

3.4 Proposed Algorithm

The proposed Learning-based Bone Cancer Detection (LbBCD) algorithm utilizes advanced deep learning techniques to accurately detect bone cancer in CT scan images, thereby enhancing early diagnosis and treatment options for patients. By preprocessing the CT scan data and training enhanced convolutional neural network (CNN) and ResNet50 models, the algorithm aims to identify cancerous patterns in bone structures with high precision. Through rigorous training, testing, and evaluation, the algorithm provides diagnostic results and performance metrics that gauge each model's effectiveness, supporting medical professionals in making informed decisions. This approach leverages the strengths of machine learning to improve diagnostic accuracy and reliability in medical imaging, ultimately contributing to more efficient and accurate cancer detection methods.

Algorithm: Learning-based Bone Cancer Detection (LbBCD)

Input: Bone CT scan dataset D

Output: Bone cancer diagnosis results R, performance statistics P, Enhanced deep learning models M (enhanced CNN and enhanced ResNet50)

1. Begin
2. D'□DataPreprocess(D)
3. (T1, T2, T3)□PrepareData(D')

Model Construction

4. Configure enhanced CNN model m1 as in Figure 2 (part of M)

```
5.      Configure enhanced ResNet50 model m2 as in Figure 2 (part of M)
6.      Compile m1
7.      Compile m2
Model Training
8.      For each model m in M
9.        m'□TrainModel(m, T1)
10.       Persist m'
11.     End For
Bone Cancer Diagnosis and Evaluation
12.     For each model m' in M'
13.       results□BoneCancerDetection(m', T2)
14.       Update R with results
15.       performance□Evaluation(results, m', T3)
16.       Update P with performance
17.     End For
18.     Print R
19.     Print P
20.     End
```

Algorithm 1: Learning-based Bone Cancer Detection (LbBCD)

The Learning-based Bone Cancer Detection (LbBCD) algorithm (Algorithm 1) is designed to leverage deep learning models for accurate bone cancer diagnosis using CT scan data. Beginning with a bone CT scan dataset (D), the algorithm's main goal is to process this data, train enhanced deep learning models, and ultimately generate diagnostic results along with performance metrics. Initially, the raw CT scan data, (D), undergoes preprocessing to produce a clean dataset (D') that is suitable for model training. The algorithm then prepares this dataset by dividing it into three subsets, (T1), (T2), and (T3), to be used respectively for model training, diagnostic testing, and performance evaluation. The algorithm employs two main models as part of its enhanced deep learning approach: an enhanced convolutional neural network (CNN) and an enhanced ResNet50, both tailored to optimize the detection of bone cancer. These models are defined and configured based on specific architecture requirements outlined in Figure 2. The enhanced CNN model, (m1), and enhanced ResNet50 model, (m2), are then compiled, enabling them to begin the training process.

For model training, each model in the collection (M), consisting of (m1) and (m2), is individually trained using the subset (T1). The training process outputs a trained model (m') for each base model, which is then stored for subsequent use in detection and evaluation. This phase ensures each model is finely tuned for bone cancer detection through the characteristics captured from the CT scan dataset. Once the models are trained, they proceed to the diagnostic stage. For each model (m') in the set of trained models (M'), the algorithm applies the model to the test data subset (T2), producing bone cancer diagnosis results that are stored in (R). This set (R) represents the diagnostic outcomes generated by each trained model. The algorithm then evaluates the diagnostic accuracy of each model. For each trained model (m'), it assesses the diagnostic results by comparing them to the known outcomes in subset (T3), generating performance metrics that are stored in (P). These metrics include measures of accuracy, sensitivity, and specificity, offering insight into each model's diagnostic capability and reliability. Finally, the algorithm outputs the diagnostic results (R) and performance statistics (P), providing a comprehensive overview of each model's effectiveness in bone cancer detection. By applying enhanced CNN and ResNet50 architectures, the LbBCD algorithm demonstrates the potential of learning-based methods for improving diagnostic accuracy in medical imaging applications.

3.5 Dataset Details

The data set is collected from [31], which has bone CT scan images. It has 5,614 cross-sectional training images and measurements in the form of ROI of the bone defect. These images are valuable for training machine-learning models to diagnose bone diseases like bone cancer or osteoporosis. The dataset is commonly used for tasks like image segmentation, classification, and detection of abnormalities within bones. The dataset includes ROI (Region of Interest) files to highlight specific areas within medical images, such as sections of bones suspected of disease or abnormalities. These files typically mark regions where a tumor or bone lesion is present, assisting models in focusing on relevant sections during training for tasks like classification or segmentation. ROI files help isolate critical areas for more accurate and efficient medical analysis.

3.6 Evaluation Methodology

Since we used a learning-based approach (supervised learning), metrics derived from the confusion matrix, shown in Figure 4, evaluate our methodology.

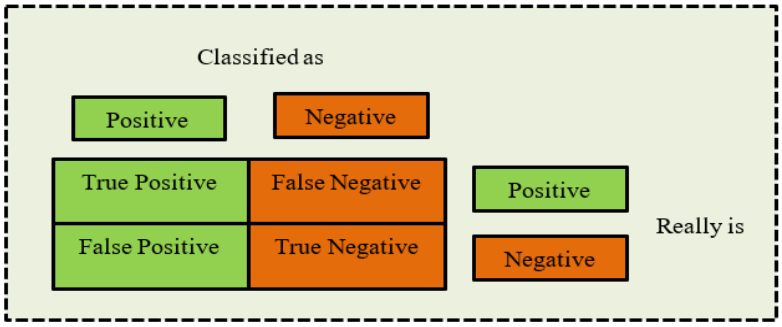

Figure 4: Confusion matrix

Based on the confusion matrix, the predicted labels of our method are compared with the ground truth to arrive at performance statistics. Eq. 1 to Eq. 4 express different metrics used in performance evaluation.

$$\text{Precision (p)} = \frac{TP}{TP+FP} \quad (1)$$

$$\text{Recall (r)} = \frac{TP}{TP+FN} \quad (2)$$

$$\text{F1-score} = 2 * \frac{(p* r)}{(p+r)} \quad (3)$$

$$\text{Accuracy} = \frac{TP+TN}{TP+TN+FP+FN} \quad (4)$$

The measures used for performance evaluation result in a value that lies between 0 and 1. These metrics are widely used in machine learning research.

4. EXPERIMENTAL RESULTS

This section presents the experimental results of the proposed system, which includes two enhanced deep-learning models. The empirical study is made with a prototype application developed using the Python programming language, which is evaluated to determine the performance of the proposed debt learning models. The experimental results with a benchmark dataset of bone seat scan images are provided in this section, along with exploratory data analysis.

Figure 5: An excerpt from the training dataset (Bone CT scan imagery) used for bone cancer detection

Figure 5 shows an excerpt from the training dataset used for bone cancer research. The dataset contains diverse samples with ground truth. The dataset contains CT scan images of bone and they contain region of interest portion of images for better training quality.

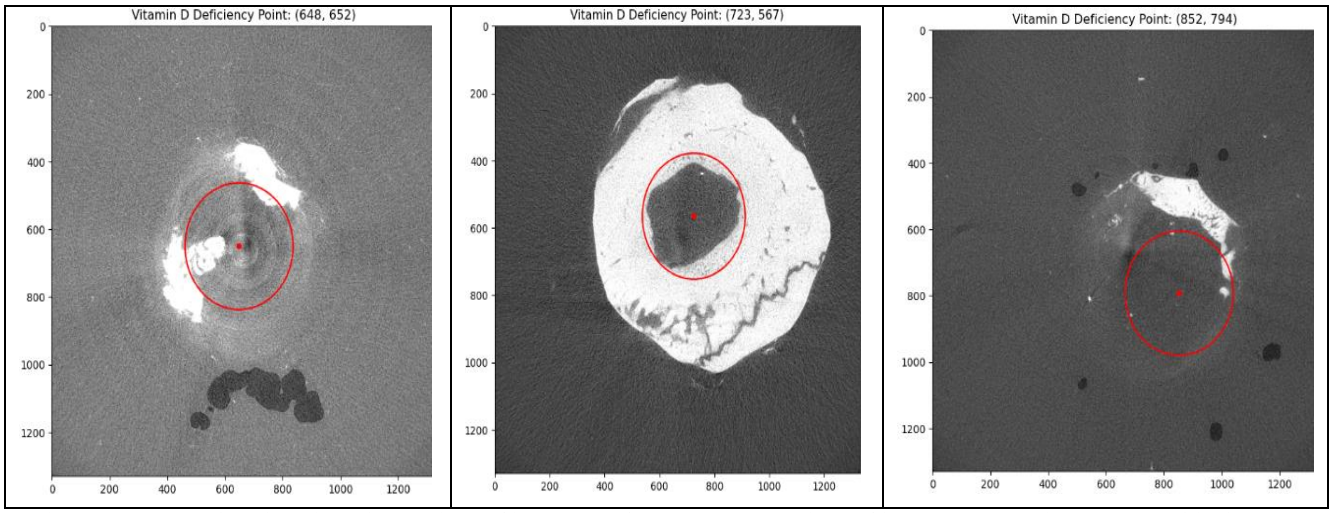

Figure 6: Results showing the region of interest after pre-processing of bone CT scan images used in bone cancer detection research

Figure 6 illustrates the results of manual image preprocessing on bone CT scan images used in bone cancer detection research. Specifically, it highlights the regions of interest (ROIs) identified for potential vitamin D deficiency. Three representative images are displayed, each showing a different ROI marked with a red circle. The ROIs are located in distinct areas of the bone, suggesting potential variations in vitamin D absorption or metabolism. These findings underscore the importance of manual image preprocessing in accurately identifying and analyzing relevant features for bone cancer detection and diagnosis.

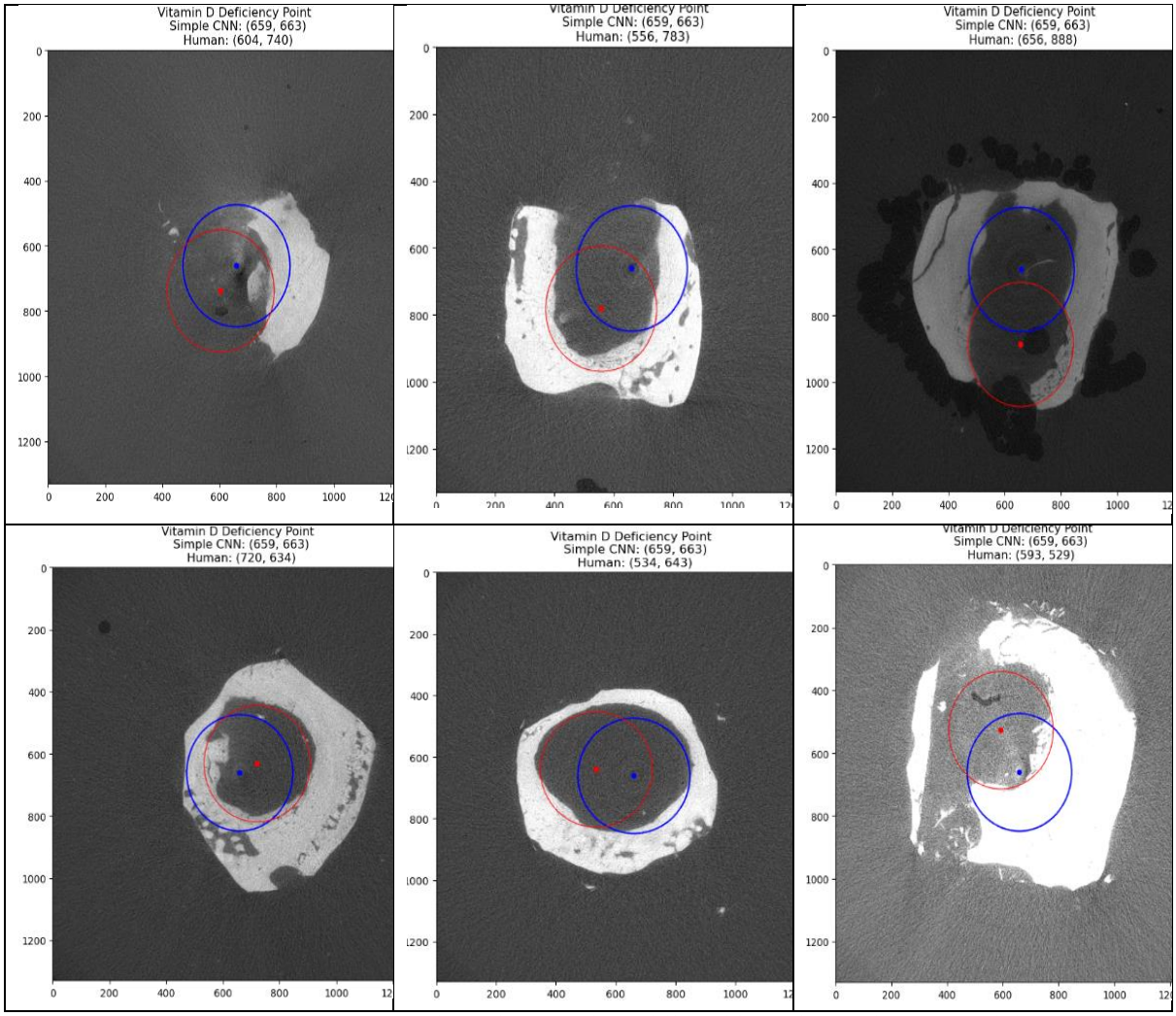

Figure 7: Bone cancer detection results exhibited by enhanced CNN model

Figure 7 illustrates the results of a bone cancer detection study using an enhanced convolutional neural network (CNN) model. The image is divided into six sections, each showcasing a different case related to vitamin D deficiency points. In each section, there are images that highlight the areas of interest where the model identified possible cancerous regions. Each image is annotated with specific metrics from the model, including the performance of a simple CNN, represented by the numbers in parentheses (e.g., Simple CNN: (659, 663)) and the human assessment (e.g., Human: (604, 740)). The circles depicted in red and blue represent the boundaries of the detected areas, indicating the regions of concern. This visual representation emphasizes the model's capability to accurately identify and localize potential bone cancer regions while also allowing for a comparison against human evaluations. The figure effectively demonstrates the application of the enhanced CNN model in medical imaging, particularly in the context of bone health assessment

Figure 8: Randomly chosen bone CT scan images used for enhanced CNN-based bone cancer diagnosis

Figure 8 illustrates the results of a bone cancer diagnosis using an enhanced convolutional neural network (CNN) model. The scatter plot compares the assessments of human experts with those generated by the CNN model for randomly selected bone CT scan images. Each point represents a specific CT scan image, where red circles denote human evaluations and a blue circle indicates the CNN model's assessment. The x-axis and y-axis likely represent specific metrics or measurements related to the bone images, such as feature values or detection scores. This visual comparison highlights the performance of the enhanced CNN model against human assessments, providing insights into the model's effectiveness in diagnosing bone cancer. The figure serves to illustrate the correlation and differences between the model's predictions and human evaluations in the context of medical imaging, emphasizing the potential of CNNs in improving diagnostic accuracy in healthcare.

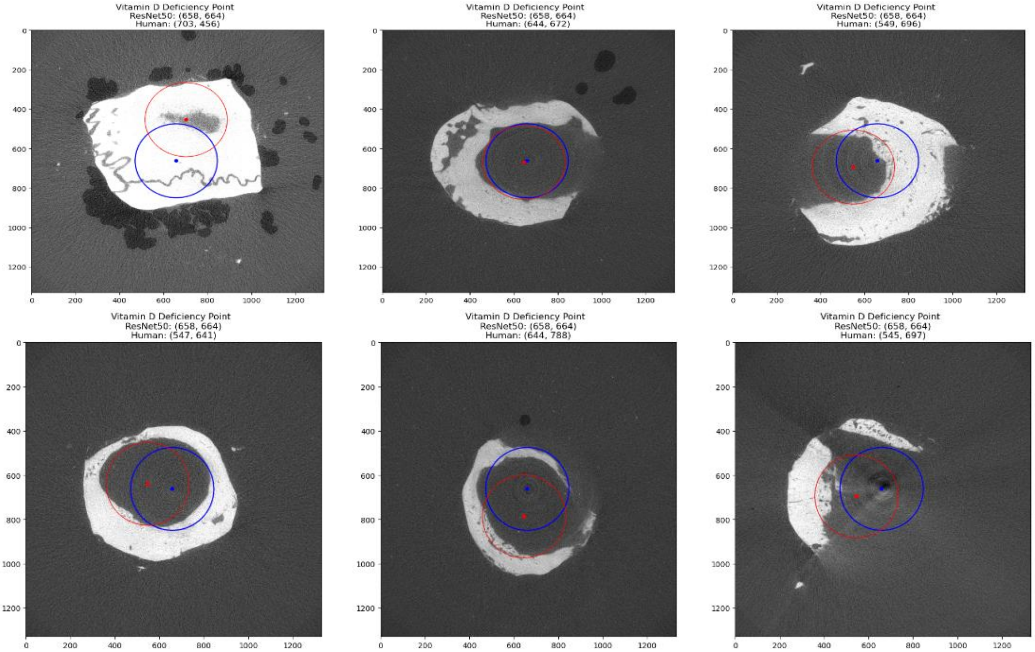

Figure 9: Bone cancer detection results exhibited by enhanced ResNet50 model

Figure 9 showcases the results of a bone cancer detection study using an enhanced ResNet50 model. These results are organized into six sections, each presenting a different case related to vitamin D deficiency points. Similar to previous figures, these images highlight areas of interest where the ResNet50 model identified potential cancerous regions in bone CT scans. Each image includes annotations detailing the performance

metrics for the ResNet50 model, indicated by the values in parentheses (e.g., ResNet50: (568, 664)), as well as the corresponding evaluations made by human experts (e.g., Human: (644, 672)). The red and blue circles represent the detected regions of concern, illustrating the model's ability to localize potential bone cancer areas effectively. This visual representation emphasizes the efficacy of the enhanced ResNet50 model in diagnosing bone cancer, allowing for a direct comparison with human assessments. The figure underlines the potential of deep learning approaches in enhancing the accuracy and reliability of medical imaging diagnostics, particularly in the context of identifying bone health issues.

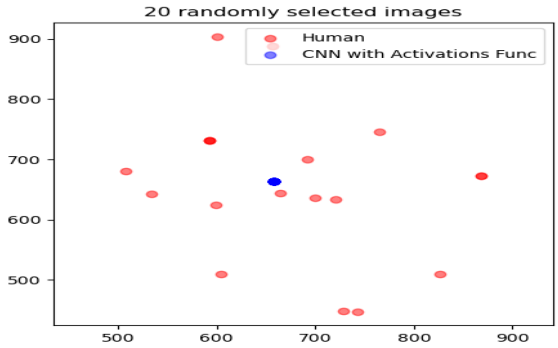

Figure 10: Randomly chosen bone CT scan images used for enhanced ResNet50-based bone cancer diagnosis

Figure 10 compares two categories of bone CT scan images utilized for enhanced ResNet50-based bone cancer diagnosis. In this visualization, red dots signify images categorized as "Human," while a blue dot represents an image assessed by the "CNN with Activations Func." The axes are marked with numeric values, suggesting a quantitative measure; however, the specific parameters represented on each axis are not labeled. A legend is included for clarity, distinguishing between the two classifications represented by different colors. This scatter plot effectively demonstrates the performance or output of the CNN model in relation to human evaluations of the same images, highlighting how the model's results align or diverge from human assessments in diagnosing bone cancer from CT scans.

Bone Cancer Detection Model	Precision	Recall	F1-Score	Accuracy
MobileNet	83.74	74.67	78.94	86.63
UNet	94.56	82.56	88.15	89.75
Enhanced CNN (Proposed)	91	98.4	94.56	90.9
Enhanced ResNet50 (Proposed)	92	88.7	90.32	92.2

Table 1: Performance comparison among bone cancer detection models

Table 1 presents a performance comparison of various bone cancer detection models, specifically focusing on key metrics: Precision, Recall, F1-Score, and Accuracy. Among the models evaluated, MobileNet achieved a precision of 83.74%, a recall of 74.67%, an F1-score of 78.94%, and an overall accuracy of 86.63%. The UNet model demonstrated significant improvement with a precision of 94.56%, a recall of 82.56%, an F1-score of 88.15%, and an accuracy of 89.75%. The Enhanced CNN model, proposed in this study, further enhanced the performance metrics, reporting a precision of 91%, a recall of 98.4%, an F1-score of 94.56%, and an accuracy of 90.9%. Lastly, the Enhanced ResNet50 model outperformed all other models, achieving a precision of 92%, a recall of 88.7%, an F1-score of 90.32%, and an accuracy of 92.2%. This comparative analysis underscores the effectiveness of the proposed enhancements in improving bone cancer detection accuracy.

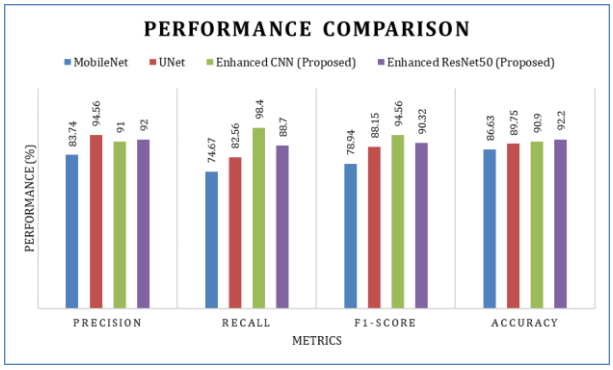

Figure 11: Performance comparison of deep learning models in bone cancer detection

Figure 11 depicts a performance comparison of four deep learning models (MobileNet, U-Net, Enhanced CNN, and Enhanced ResNet50) in bone cancer detection. The models are evaluated based on four metrics: Precision, Recall, F1-Score, and Accuracy. The results indicate that the Enhanced ResNet50 model outperforms the others in all metrics, achieving the highest precision (94.56%), recall (98.4%), F1-Score (90.32%), and accuracy (92%). The Enhanced CNN also shows promising results, with high precision (94.56%) and recall (98.4%). However, it falls slightly behind in F1-Score and accuracy compared to the Enhanced ResNet50. The MobileNet and U-Net models exhibit lower performance overall, especially in terms of recall. MobileNet, in particular, struggles with recall, achieving only 74.67%. The Enhanced ResNet50 model emerges as the most effective deep learning model for bone cancer detection based on the given metrics. It demonstrates superior performance in accurately identifying and classifying bone cancer cases.

5. DISCUSSION

Technological innovations, such as artificial intelligence (AI), have the potential to solve problems across various real-world applications. In the healthcare industry, traditional approaches can be enhanced with AI-enabled methodologies, especially in areas like disease diagnosis and medical document classification. Machine learning and deep learning models are widely utilized for processing medical data. Various medical imaging modalities are employed to diagnose different diseases. For all these modalities, deep learning models, particularly convolutional neural networks (CNNs), have proven effective in extracting and analyzing features from images. However, our research indicates that deep learning models need further improvement for different imaging modalities in order to enhance their prediction performance. In this study, we focus on using bone CT scan images to facilitate the early detection of bone cancer. Early detection is crucial, as it significantly impacts treatment procedures and patient outcomes. Therefore, this research holds considerable importance. We enhanced both the CNN model and the ResNet-50 model to improve their performance in medical data analytics, specifically concerning bone CT scan images. Our empirical study, which utilized a benchmark dataset, demonstrated the superior performance of these enhanced deep-learning models. Consequently, the proposed deep learning framework can be integrated into healthcare applications for the automatic screening of bone cancer. However, it is important to note that the proposed system has certain limitations, as discussed in Section 5.1.

5.1 Limitations

The proposed system presented in this paper has some limitations. It was tested and evaluated using only one imaging modality: CT scan images. Specifically, only bone CT images were utilized for the evaluation of the system. However, in real-world scenarios, MRI images may also need to be processed. Another significant limitation is that the dataset consists of a finite number of samples, lacking diversity in both the samples and the volumes. This lack of variety may hinder the generalization of the findings. Furthermore, the proposed system relies exclusively on CNN-based models, whereas other deep learning models could potentially be explored to enhance the system's performance.

6. CONCLUSION AND FUTURE WORK

We propose a deep learning framework that employs advanced convolutional neural network (CNN) models for automatically screening bone cancer. Our approach enhances both the CNN model and the ResNet-50 model, which are integral components of this framework. Additionally, we have introduced an algorithm called Learning-based Bone Cancer Detection (LbBCD) to optimize the use of these enhanced models and improve bone cancer detection efficiency. Our research focuses on a Region of Interest (ROI) approach to enhance the screening process for bone cancer. Using the Bone CT Scan dataset as a benchmark, our empirical study demonstrated that the proposed deep learning framework, incorporating the enhanced CNN and ResNet-50 models, achieved remarkable performance. Specifically, the enhanced CNN model attained an accuracy of 90.90%, while the enhanced ResNet-50 model achieved an accuracy of 92.20%, outpacing other state-of-the-art deep learning models. Thus, this proposed system can be integrated into healthcare applications for the automatic screening of bone cancer, contributing to a clinical decision support system for healthcare professionals. In our future work, we intend to enhance our framework by incorporating long short-term memory models, possibly using a hybrid approach to leverage cancer detection performance further. Another important direction for future research is to utilize explainable AI to improve the proposed deep learning framework.

REFERENCES

[1] Yun Feng Zhang, Chuan Zhou, Sheng Guo, Chao Wang, Jin Yang, Zhi-Jun Yang, Rong Wang, Xu Zhang, and Feng-Hai Zhou. (2024). Deep learning algorithm-based multimodal MRI radiomics and pathomics data improve prediction of bone metastases in prima. Springer. 150(78), pp.1-13. https://doi.org/10.1007/s00432-023-05574-5

[2] SHTWAI ALSUBAI, ASHIT KUMAR DUTTA, FAISAL ALGHAYADH, RAFIULLA GILKARAMENTHI, MOHAMAD KHAIRI ISHAK, FATEN KHALID KARIM, SAMEER ALSHETEWI, AND SAMIH M. MOSTAFA. (2024). Group Teaching Optimization With Deep Learning-Driven Osteosarcoma Detection Using Histopathological Images. IEEE. 12, pp.34089 - 34098. http://DOI:10.1109/ACCESS.2024.3371518

[3] E. Rachmawati, M. D. Sulistiyo, and D. B. Nugraha. (2024). Leveraging Model Scaling and Butterfly Network in the Bone Scan Image Segmentation. Springer. 17(92), pp.1-18. https://doi.org/10.1007/s44196-024-00453-4

[4] Ali Ataei, Florieke Eggermont, Nico Verdonschot, Nikolas Lessmann, and Esther Tanck. (2024). The effect of deep learning-based lesion segmentation on failure load calculations of metastatic femurs using finite element analysis. Elsevier. 179, pp.1-9. https://doi.org/10.1016/j.bone.2023.116987

[5] Sushopti Gawade, Ashok Bhansali, Kshitij Patil, and Danish Shaikh. (2023). Application of the convolutional neural networks and supervised deep-learning methods for osteosarcoma bone cancer detec. Elsevier. 3, pp.1-9. https://doi.org/10.1016/j.health.2023.100153

[6] Yuchao Xiong, Wei Guo, Zhiping Liang, Li Wu, Guoxi Ye, Ying-ying Liang, Chao Wen, Feng Yang, Song Chen, Xu-wen Zeng, and Fan Xu. (2023). Deep learning–based diagnosis of osteoblastic bone metastases and bone islands in computed tomograph images: a multice. Springer. 33, pp.1-10. https://doi.org/10.1007/s00330-023-09573-5

[7] Manjula Devi Ramasamy, Rajesh Kumar Dhanaraj, Subhendu. Kumar Pani, Rashmi Prava Das, Ali Akbar Movassagh, Mehdi Gheisari, Yang Liu, and P. Porkarf , Sabitha Banu (2023). An improved deep convolutionary neural network for bone marrow cancer detection using image processing. Elsevier. 38, pp.1-9. https://doi.org/10.1016/j.imu.2023.101233

[8] Nasibeh Mohseninia, Nazanin Zamani-Siahkali, Sara Harsini, Ghasemali Divband, Christian Pirich, and Mohsen Beheshti. (2023). Bone Metastasis in Prostate Cancer: Bone Scan Versus PET Imaging. Elsevier. 54(1), pp.97-118. https://doi.org/10.1053/j.semnuclmed.2023.07.004

[9] Marwa Afnouch, Olfa Gaddour, Yosr Hentati, Fares Bougourzi, Mohamed Abid, Ihsen Alouani, Abdelmalik Taleb Ahmed. (2023). BM-Seg: A new bone metastases segmentation dataset and ensemble of CNN-based segmentation approach. Elsevier. 228, pp.1-34. https://doi.org/10.1016/j.eswa.2023.120376

[10] Dapeng Wang, Yan Sun, Xing Tang, Caijun Liu, and Ruiduan Liu. (2023). Deep learning-based magnetic resonance imaging of the spine in the diagnosis and physiological evaluation of spinal meta. Elsevier. 40, pp.1-6. https://doi.org/10.1016/j.jbo.2023.100483

[11] Sushopti Gawade, Ashok Bhansali, Kshitij Patil, and Danish Shaikh. (2023). Application of the convolutional neural networks and supervised deep-learning methods for osteosarcoma bone cancer detection. Elsevier. 3, pp.1-9. https://doi.org/10.1016/j.health.2023.100153

[12] EATEDAL ALABDULKREEM, MUHAMMAD KASHIF SAEED, SAUD S. ALOTAIBI, RANDA ALLAFI, ABDULLAH MOHAMED, AND MANAR AHMED HAMZA. (2023). Bone Cancer Detection and Classification Using Owl Search Algorithm With Deep Learning on X-Ray Images. IEEE. 11, pp.109095 - 109103. http://DOI:10.1109/ACCESS.2023.3319293

[13] Sophia S. Goller, Sarah C. Foreman, Jon F. Rischewski, Jürgen Weißinger, Anna-Sophia Dietrich, David Schinz, Robert Stahl, Johanna Luitjens, Sebastian Siller, Vanessa F. Schmidt, Bernd Erber, Jens Ricke, Thomas Liebig, Jan S. Kirschke, Michael Dieckmeyer, Alexandra S. Gersing. (2023). Differentiation of benign and malignant vertebral fractures using a convolutional neural network to extract CT-based texture features. Springer. 32, pp.1-7. https://doi.org/10.1007/s00586-023-07838-7

[14] Abdalla Ibrahim, Akshayaa Vaidyanathan, Sergey Primakov, Flore Belmans, Fabio Bottari, Turkey Refaee, Pierre Lovinfosse, Alexandre Jadoul, Celine Derwael, Fabian Hertel, Henry C. Woodruf, Helle D. Zacho, Sean Walsh, Wim Vos, Mariaelena Occhipinti, François-Xavier Hanin, Philippe Lambin, Felix M. Mottaghy, and Roland Hustinx. (2023). Deep learning based identification of bone scintigraphies containing metastatic bone disease foci. Springer. 23(12), pp.1-9. https://doi.org/10.1186/s40644-023-00524-3

[15] Hanna Leena Halme, Toni Ihalainen, Olli Suomalainen, Antti Loimaala, Sorjo Mätzke, Valtteri Uusitalo, Outi Sipilä, and Eero Hippeläinen. (2022). Convolutional neural networks for detection of transthyretin amyloidosis in 2D scintigraphy images. Springer. 12(27), pp.1-11. https://doi.org/10.1186/s13550-022-00897-9

[16] Priti Bansal, Kshitiz Gehlot, Abhishek Singhal, and Abhishek Gupta. (2022). Automatic detection of osteosarcoma based on integrated features and feature selection using binary arithmetic optimization algorithm. Springer. 81, pp.1-28. https://doi.org/10.1007/s11042-022-11949-6

[17] Ricarda Hinzpeter, Livia Baumann, Roman Guggenberger, Martin Huellner, Hatem Alkadhi, Bettina Baessler. (2022). Radiomics for detecting prostate cancer bone metastases invisible in CT: a proof-of-concept study. Springer. 32, pp.1-10. https://doi.org/10.1007/s00330-021-08245-6

[18] DEEPIKA KUMAR, NIKITA JAIN, AAYUSH KHURANA, SWETA MITTAL, SURESH CHANDRA SATAPATHY, ROMAN SENKERIK, AND JUDE D. HEMANTH. (2020). Automatic Detection of White Blood Cancer From Bone Marrow Microscopic Images Using Convolutional Neural Networks. IEEE. 8, pp.142521 - 142531. http://DOI:10.1109/ACCESS.2020.3012292

[19] Sarah Lindgren Belal, May Sadik, Reza Kaboteh, Olof Enqvist, Johannes Ulén, Mads H. Poulsen, Jane Simonsen, Poul F. Høilund-Carlsen, Lars Edenbrandt, and Elin Trägårdh. (2019). Deep learning for segmentation of 49 selected bones in CT scans: First step in automated PET/CT-based 3D quantification of skeletal metastases. Elsevier. 113, pp.89-95. https://doi.org/10.1016/j.ejrad.2019.01.028

[20] Papandrianos, Nikolaos; Papageorgiou, Elpiniki I. and Anagnostis, Athanasios . (2020). Development of Convolutional Neural Networks to identify bone metastasis for prostate cancer patients in bone scintigraphy. Annals of Nuclear Medicine, 34, pp.1-9. http://doi:10.1007/s12149-020-01510-6

[21] Shao, Xiaoguang; Zhang, Heng; Wang, Yanqing; Qian, Hongyang; Zhu, Yinjie; Dong, Baijun; Xu, Fan; Chen, Na; Liu, Shupeng; Pan, Jiahua and Xue, Wei . (2020). Deep convolutional neural networks combine Raman spectral signature of serum for prostate cancer bone metastases screening. Nanomedicine: Nanotechnology, Biology and Medicine, 29, pp.1-25. http://doi:10.1016/j.nano.2020.102245

[22] Bhukya Jabber; M. Shankar; P. Venkateswara Rao; Azmira Krishna and Cmak Zeelan Basha;. (2020). SVM Model based Computerized Bone Cancer Detection . 2020 4th International Conference on Electronics, Communication and Aerospace Technology (ICECA), pp.1-5. http://doi:10.1109/iceca49313.2020.9297624

[23] Noguchi, Shunjiro; Nishio, Mizuho; Yakami, Masahiro; Nakagomi, Keita and Togashi, Kaori . (2020). Bone segmentation on whole-body CT using convolutional neural network with novel data augmentation techniques. Computers in Biology and Medicine, 121, pp.1-9. http://doi:10.1016/j.compbiomed.2020.103767

[24] Anisuzzaman, D. M., Barzekar, H., Tong, L., Luo, J., & Yu, Z. (2021). A deep learning study on osteosarcoma detection from histological images. Biomedical Signal Processing and Control, 69, pp.1-10. http://doi:10.1016/j.bspc.2021.102931

[25] Fang, Yijie; Li, Wei; Chen, Xiaojun; Chen, Keming; Kang, Han; Yu, Pengxin; Zhang, Rongguo; Liao, Jianwei; Hong, Guobin and Li, Shaolin . (2020). Opportunistic osteoporosis screening in multi-detector CT images using deep convolutional neural networks. European Radiology, 31, pp.1-12. http://doi:10.1007/s00330-020-07312-8

[26] Aoki, Y., Nakayama, M., Nomura, K., Tomita, Y., Nakajima, K., Yamashina, M., & Okizaki, A. (2020). The utility of a deep learning-based algorithm for bone scintigraphy in patient with prostate cancer. Annals of Nuclear Medicine, 34(12), pp.926–931. http://doi:10.1007/s12149-020-01524-0

[27] B.S Vandana and Sathyavathi R. Alva;. (2021). Deep Learning Based Automated tool for cancer diagnosis from bone histopathology images . 2021 International Conference on Intelligent Technologies (CONIT), pp.1-8. http://doi:10.1109/conit51480.2021.9498367

[28] Samira Masoudi; Sherif Mehralivand; Stephanie A. Harmon; Nathan Lay;Liza Lindenberg; Esther Mena; Peter A. Pinto; Deborah E. Citrin; James L. Gulley; Bradford J. Wood; William L. Dahut; Ravi A. Madan; Ulas Bagci; Peter L. Choyke and Baris Turkbey;. (2021). Deep Learning Based Staging of Bone Lesions From Computed Tomography Scans. IEEE Access, 9, pp. 87531 - 87542. http://doi:10.1109/access.2021.3074051

[29] Jingteng He, and Xiaojun Bi. (2024). Automatic classification of spinal osteosarcoma and giant cell tumor of bone using optimized DenseNet. Elsevier. 46, pp.1-8. https://doi.org/10.1016/j.jbo.2024.100606

[30] Ki-Seong Park, and Hee-Seung Henry Bom. (2024). Recent updates on applications of Artificial Intelligence for Nuclear Medicine professionals: bone scintigraphy. Springer. 58, pp.1-5. https://doi.org/10.1007/s13139-023-00833-2

[31] CT Scan Dataset. Retrieved from https://www.kaggle.com/datasets/chzpan/bone-lab/data